Monte Carlo Studies of an Idealized Model of a Lipid-Water System†

Mariusz Milik,‡ Jeffrey Skolnick,*,‡ and Andrzej Kolinski‡,§

Department of Molecular Biology, The Scripps Research Institute, 10666 N Torrey Pines Rd., La Jolla, California 92037, and Department of Chemistry, University of Warsaw, Pasteura 1, Warsaw, Poland
(Received: September 30, 1991)

Employing Monte Carlo dynamics, the equilibrium and dynamic properties of lipid-water systems are studied in the context of a diamond lattice realization. The model faithfully describes the lipid molecule geometry and reproduces the essential physical properties of real membranes. These include the phase transitions from quasi-crystalline phase ↔ liquid bilayer ↔ nonbilayer, quasi-hexagonal phase ↔ dissolved liquid solution. Furthermore, the structure, ordering, and dynamics of the model liquid bilayer are in good accord with experiment, and the values of segmental ordering parameters are close to those obtained from NMR data. Due to the diamond lattice representation and a very efficient simulation algorithm, the intermediate distance scale dynamic features of the water-lipid system could be examined; these include lateral diffusion in the bilayer, the formation of a nonbilayer phase, the transbilayer diffusion of the lipid molecule, and the diffusion of a lipid molecule in the water phase. The present model can be also used to generate initial configurations for more detailed molecular (or Brownian) dynamics studies of lipid-water systems.

1. Introduction

Due to their great biological and medical importance, the structure and dynamics of lipid-water systems have been the object of increased attention.[1-3] This is reflected in the many experimental and theoretical methods applied to the investigation of the molecular structure, dynamics, and related biological properties of these systems.[3-7] Because of their inherent complexities, molecular dynamics and Monte Carlo studies of model systems could be extremely helpful in elucidating the dynamic properties, the stability, and the phase transitions of mono- and bilayers.[8-18]

In principle, molecular dynamics simulations provide the most realistic, physical description of the system and have been employed to obtain realistic information about the physical and thermodynamic parameters of a single alkane chain or a small ensemble of chains.[10-12] However, even for these small and in many cases simplified systems, it is difficult to obtain trajectories longer than hundreds of picoseconds. Simulations on this time scale can give insights into the internal dynamics of the alkane chain, as well as the short-range structural transitions in the mono- or bilayer. However, they are insufficient to study the intermediate- or large-scale dynamic and static properties of large ensembles of lipids. This is especially true since some structural changes in real bilayers are very cooperative and are characterized by large relaxation times.[19,20]

The simplest method to sample the long-time behavior of large systems is to employ a lattice model of the bilayer and to simulate the motion using Monte Carlo dynamics. With a proper choice of the lattice, one can obtain a reasonable geometric representation of the lipid molecules. The lattice provides an integer representation for the molecules which allows for the maximal speed-up of the algorithm relative to the off-lattice case. Finally, sampling by dynamic Monte Carlo sets the elemental time unit on the order of the mean conformational isomerization time, which is typically on the order of 0.1-1 ns.

The present model extends to more complicated systems our earlier study of a monolayer consisting of lattice chains, one of whose ends is constrained to lie near an interface.[16,21,22] There, we found that the static and dynamic properties of those model chains are similar to those observed in a real bilayer. Encouraged by these initial results, here we employ a more realistic molecular geometry as well as the exact topology of the lipid molecules in the model bilayer and investigate a number of their equilbrium and dynamic properties. The foundation of this work is the assumption that hydrophobic interactions between the alkane chains and the availability of multiple internal rotational isomeric states are the main driving force for the structural transitions seen in lipid-water systems.

We have opted for a tetrahedral lattice approximation to represent the accessible conformations of each molecule and the allowed intermolecular arrangements in the bilayer. In spite of lattice simplifications, the model exhibits many features which can be related to the properties of real systems. In particular, the model provides a good description of the structure and dynamics of the lipid-water system over a wide temperature range. Moreover, on the level of the united-atom representation and contact-type interactions, we have the possibility of following the behavior of the system from the crystal phase through the liquid-crystal and quasi-hexagonal phases to an isotropic liquid. To the best our knowledge, this is first time that all the features of the lipid-water system have been depicted by one universal model. We find that the results of the simulations are always qualitatively consistent with experiment.

Apart from their intrinsic interest, an important reason why we have begin a study of this class of models is that they provide a basis for the examination of more complicated problems associated with lipid-cholesterol and lipid-protein interactions in biological membranes. These problems require the use of large assemblies of lipids and very long simulation times. One such

† This paper is dedicated with gratitude and respect to Professor Marshall Fixman on the occasion of his 60th birthday.

‡ The Scripps Research Institute.

§ University of Warsaw.

(1) Israelachvili, J. N.; Marcelja, S.; Horn, R. G. *Q. Rev. Biophys.* **1980**, *13*, 121.
(2) Quinn, P. J. In *Subcellular Biochemistry*; Harris, J. R., Etemadi, A.-H., Eds.; Plenum Press: New York, 1986; Vol. 14, p 25.
(3) Biltonen, R. L. *J. Chem. Thermodyn.* **1990**, *22*, 1.
(4) Gulik-Krzywicki, T.; Rivas, E.; Luzzati, V. *J. Mol. Biol.* **1967**, *27*, 303.
(5) Luzzati, V.; Tardieu, A. *Annu. Rev. Phys. Chem.* **1974**, *25*, 79.
(6) Caffrey, M. *Biochemistry* **1985**, *24*, 4826.
(7) Siegel, D. P.; Burns, J. L.; Chestnut, M. H.; Talmon, Y. *Biophys. J.* **1989**, *56*, 161.
(8) Fraser, D. P.; Chantrell, R. W.; Melville, D.; Tildesley, D. J. *Liq. Cryst.* **1988**, *3*, 423.
(9) Freire, E.; Snyder, B. *Biochim. Biophys. Acta* **1980**, *600*, 643.
(10) Harris, J.; Rice, S. A. *J. Chem. Phys.* **1988**, *89*, 5898.
(11) Pleog van der, P.; Berendsen, H. J. C. *J. Chem. Phys.* **1982**, *76*, 3271.
(12) De Loof, H.; Harvey, S. C.; Segrest, J. P.; Pastor, R. W. *Biochemistry* **1991**, *30*, 2099.
(13) Jayaram, B.; Mezei, M.; Beveridge, D. L. *J. Comput. Chem.* **1987**, *8*, 917.
(14) Larson, R. G. *J. Chem. Phys.* **1988**, *89*, 1642.
(15) Rey, A.; Kolinski, A.; Skolnick, J.; Levine, Y. K. *J. Chem. Phys.*, in press.
(16) Milik, M.; Kolinski, A.; Skolnick, J. *J. Chem. Phys.* **1990**, *93*, 4440.
(17) Owenson, B.; Pratt, L. R. *J. Phys. Chem.* **1984**, *88*, 2905.
(18) Scott, H. L. *Biochim. Biophys. Acta* **1977**, *469*, 264.
(19) Cevc, G.; Marsh, D. *Phospholipid Bilayers—Physical Principles and Models*; John Wiley & Sons: New York, 1987.
(20) Marsh, D. *Chem. Phys. Lipids* **1991**, *57*, 109.
(21) Milik, M.; Orszagh, A. *Polymer* **1989**, *30*, 681.
(22) Milik, M.; Orszagh, A. *Polymer* **1990**, *31*, 506.

0022-3654/92/2096-4015$03.00/0

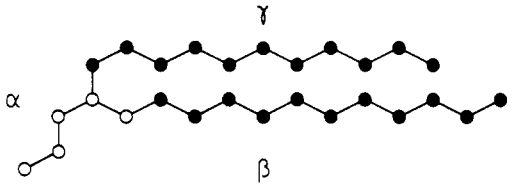

Figure 1. Tetrahedral lattice representation of the model of a lipid molecule. The model consists of a hydrophilic α-chain (open circles) and two hydrophobic alkane chains (solid circles).

realization is an ongoing study of the folding of a lattice model of a short polypeptide in a lipid bilayer. This will be the subject of a future publication. Furthermore, since Monte Carlo lattice simulations generate states at thermal equilibrium, this method provides excellent initial configurations (at various temperatures) for more exact off-lattice Monte Carlo and, subsequently, for molecular or Brownian dynamics simulations of the bilayer. This will allow the study of the character of the smaller distance scale and shorter time properties.

The outline of the remainder of the paper is as follows. Section 2 discusses the model in detail and the Monte Carlo dynamics algorithm used to move the molecules about. Section 3 presents the results of the equilibrium and dynamic properties of these model systems. Finally, section 4 summarizes the conclusions of the present work and outlines the directions of future research.

2. Method of Simulation

2.1. Description of the Model Molecule. The lipid molecule selected for the present simulation is dilauroylphosphatidylethanolamine (DLPE), whose tetrahedral lattice representation is given in Figure 1. It consists of a hydrophilic α-chain and two hydrophobic (alkane) chains, i.e. the β-chain and the γ-chain.[23,24] The open circles correspond to the polar (hydrophilic) fragment of the lipid, and the solid circles correspond to the backbone of the hydrophobic chains. Thus, the united-atom representation is adopted. All the bonds in the model molecule are of the same length, and all the angles correspond to the tetrahedral valence angle. The set of allowed dihedral angles corresponds to the rotational isomeric states of a bond in an alkane molecule (two gauche states and one trans state).

The model molecule can undergo various conformational transitions. As schematically shown in Figure 2a,b, all the chain ends can move by single-bond and two-bond rearrangements. The middle segments of the β- and γ-chains can move by propagation of gauche conformations down the chain. The crankshaft micromodification employed to achieve this is shown in Figure 2c.

The movement of the branch point and the α-chain requires separate treatment. Three types of micromodifications of the model molecule conformation are used. The first one (Figure 2d) is the snakelike move of the entire contour of the β- and γ-chains. The branch point moves simultaneously by one bond with an appropriate change of the α-chain conformation. The second kind of move (Figure 2e) consists of the rotation around the first bond of the α-chain from the branch point. Both hydrophobic chains interchange their positions with appropriate displacements down their contours. Figure 2f illustrates the last type of branch point rearrangement which is a four-bond flip of this point and which conserves the rest of β- and γ-chains. The α-chain is pulled along with the movement of the branch point. The motion of the entire model molecule is realized by a sequence of the above micromodifications.

The configurational energy of the molecule consists of both long-range and short-range interactions. The long-range interactions are defined by a square-well potential between nonbonded pairs of united atoms (beads). Taking into account that multiple occupancy of any lattice site is forbidden, the energy term ϵ_h is associated with every nonbonded hydrophobic pair separated by

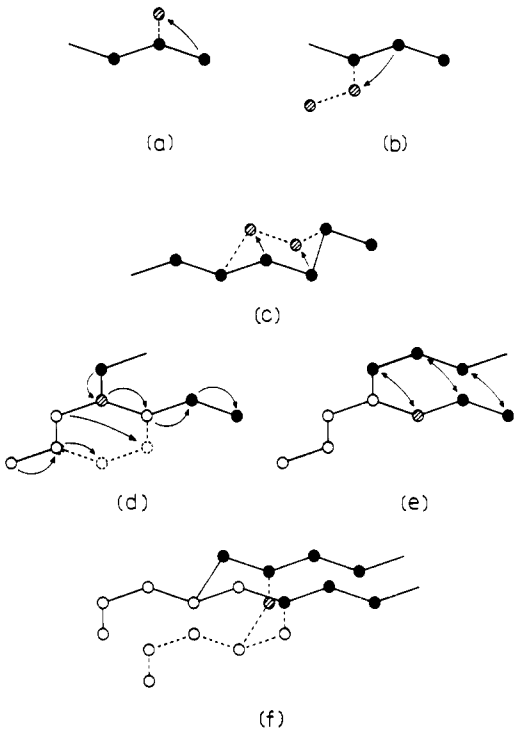

Figure 2. Set of elemental micromodifications used in the Monte Carlo dynamics procedure: (a) Single-bond move of the chain ends. (b) Two-bond move of the chain ends. (c) The crankshaft modification of internal segments of the alkane chains. This move propagates the "gauche" defect along the chain. (d) Snakelike move of the entire contour of the alkane chains. The branchpoint moves along with a change of the conformation of the α-chain. (e) Rotation of whole lipid molecule around its axis of symmetry. This move changes the branch point geometrical coordinates. (f) Four-bond move of the branch point with rearrangement of the α-chain.

a distance equal to the bond length (lattice vector). The ϵ_h term may be considered to be a potential of mean force representing hydrophobic interactions. It is included only for the β- and γ-chains (solid beads in Figure 1). Thus, the hydrophilic α-chain is taken to be inert. However, this produces an effective, repulsive potential between hydrophilic and hydrophobic chains. Short-range interactions are related to the energy ϵ_{tg} of gauche states relative to trans states of the chain backbone. In the present simulation, $|\epsilon_{tg}/\epsilon_h| = 2.0$. This is an arbitrary choice; however, the value 2.0 seems to be quite reasonable for alkane chains.

2.2. The Model of Bilayer. The model membrane consists of the collection of lipid molecules described above. At low temperature, the system is highly ordered, and the hydrophobic chains in their extended, all-trans, conformation are close packed inside the bilayer. The hydrophilic α-chains are exposed to the solvent surrounding the membrane. The solvent molecules are not simulated directly. It is assumed that every lattice site not occupied by a lipid molecule represents the solvent. A schematic illustration of the model bilayer is given in Figure 3a. It should be noted that, due to the nature of the diamond lattice, the angle between the XY plane and the chain axis is not equal to 90°, as suggested by the figure. Looking down the X axis direction, this angle equals 45°, and only a part of bilayer section is drawn for the sake of clarity. The entire Monte Carlo (MC) box in most simulations is a cuboid of size 48 × 48 × 64 (Figure 3b). Periodic boundary conditions are superimposed in the X, Y, and Z directions. As depicted in Figure 3b, at the beginning of the simulation the model bilayer is placed within the central layer of the box. The size of the MC box is certainly large enough to study local arrangements at various temperatures as well as to study the lateral cooperative displacement of lipid molecules. However, the model system is too small to say anything about oscillations in curvature of the entire membrane. The last statement is related to the presence of periodic boundary conditions, which act to make the membrane surfaces too rigid.

(23) Hitchcock, P. B.; Mason, R.; Thomas, K. M.; Shipley, G. G. *Proc. Natl. Acad. Sci. U.S.A.* **1974**, *71*, 3036.
(24) Hauser, H.; Pascher, I.; Pearson, R. H.; Sundell, S. *Biochim. Biophys. Acta* **1981**, *650*, 21.

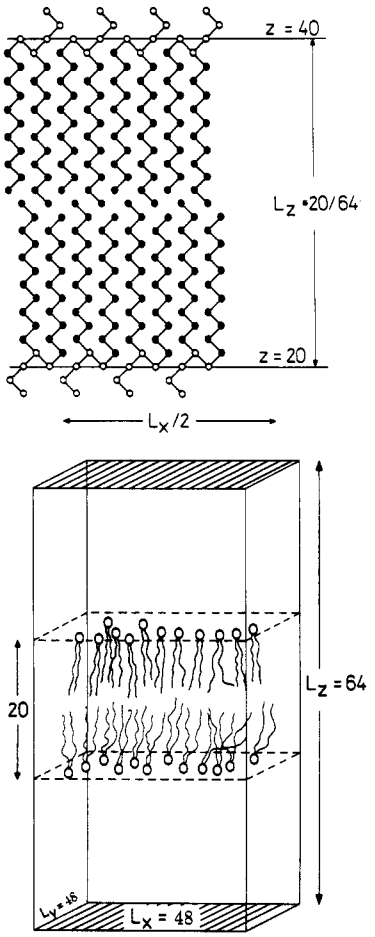

Figure 3. Initial configuration of the model of bilayer: (a, top) schematic illustration of an initial configuration of model lipid molecules; (b, bottom) schematic representation of the Monte Carlo box, where the model bilayer is placed in the central layer of the box.

The model system is studied at a surface density $\rho = 0.80$. This is achieved by randomly removing 20% of the molecules from the close-packed system shown schematically in Figure 3a. As a result, the model system consists of 230 molecules, i.e., 460 hydrophobic chains per MC box.

2.3. Monte Carlo Simulations. The temperature of the model system is defined in the conventional way, $T^* = k_B T/\epsilon_h$ with k_B equal to Boltzmann's constant. The configurational energy of the system is counted as a sum of short-range and long-range interactions

$$E_c = n_c\epsilon_h + n_g\epsilon_{tg} \quad (1)$$

where n_c is the number of contacts between hydrophobic beads and n_{tg} is the number of gauche conformational states in all the chains.

The standard asymmetric Metropolis sampling scheme is used in the simulation procedure. A random number generator chooses the chain and the bead. Then, a micromodification is attempted. If the "old" state energy is E_i and that of the new state is characterized by energy E_j, one may define the transition probability by

$$p_{ij} = \exp\{-[(E_j - E_i)/k_B T]\} \quad (2)$$

The above step has to be iterated many times. The simulation starts from a low-temperature, ordered state. Every production run is preceded by a suitable equilibration period (on the order of 10^6 steps per bead). This equilibration procedure is repeated after every change in temperature. In this way, we obtain estimates of various properties of the model system over a wide range of reduced temperatures from $T^* = 0.7$ to $T^* = 2.0$. The efficiency of the lattice modeling algorithms for dense systems with strong interactions is usually not great and changes with temperature and structure of the model system.

TABLE I: Fraction of Accepted Micromodifications as a Function of the Reduced Temperature Parameter

temp	no. of MC steps	fraction of accepted end moves	fraction of accepted crankshaft moves	fraction of accepted head moves
0.7	3.75×10^6	2.2	0.075	43.25
0.8	4.25×10^6	3.28	0.175	41.92
0.9	3.25×10^6	3.38	0.203	43.64
1.0	4.25×10^6	6.28	0.326	40.96
1.1	4.75×10^6	8.24	0.621	40.11
1.2	5.50×10^6	15.27	1.52	28.98
1.3	3.50×10^6	20.97	3.09	46.67
1.4	4.50×10^6	26.92	4.46	43.89
1.5	5.00×10^6	31.85	5.84	48.45
1.6	4.00×10^6	36.40	7.20	51.95
1.7	1.25×10^6	40.16	8.71	57.37
1.8	1.25×10^6	42.59	9.57	58.15
1.9	1.25×10^6	44.90	10.40	58.52
2.0	1.25×10^6	46.90	11.15	58.72

Table I shows the percentage of accepted moves obtained in the present simulations. As one can see, the mobility of head groups is very large and weakly correlated with temperature. This is consistent with expectation, because of the small local density in the hydrophilic layer of the membrane. The probability of a crankshaft move (a very important move in this simulation, which propagates "gauche" conformations; see Figure 2c) is very small in the low-temperature, ordered system. This is due to the high system density and the low concentration of "gauche" defects in the ordered system. Note that the "gauche" state of a chosen bead is a necessary condition for this move. The percentage of accepted gauche propagation moves increases with temperature because of the increase in system disorder. One suprising feature of Table I is the minimum in the mobility of the head groups near $T^* = 1.2$. We will try to explain this effect below on the basis of structural changes in the system. The mobility of the hydrophobic tails grows monotonically due to both changes in local density in the hydrophobic region of the system and the increase in the number of gauche states which modifies the probability of acceptance of a move (see eq 2).

A fundamental question is whether the mobility of the system at low temperature is large enough to obtain an equilibrated state. If 0.1% of the moves are accepted in a simulation of ca. 4×10^6 MC steps (the mean simulation time for low-temperature systems), we have 4000 accepted moves per bead during the simulation. This is sufficient to equilibrate a short-chain system.

3. Results

3.1. Equilibrium Properties. The first computational experiment consisted of a set of independent simulations of the model bilayer systems at reduced temperatures T^* between 0.7 and 2.0. The goal of these simulations was to observe changes in the equilibrium structure of the model bilayer as a function of temperature. Every simulation started from the same, quasi-crystalline state at a density $\rho = 0.80$. After thermalization, the systems reached an equilibrium state and then remained stable. Figure 4 presents representative trajectories of the average number of hydrophobe–hydrophobe contacts at temperatures 0.8, 1.0, 1.2, 1.4, and 2.0. The time scale is in Monte Carlo steps. One MC step is the time when the algorithm tries to move every unit in every molecule. The initial, highly nonequilibrium fragments of the trajectories were rejected and not considered in calculations of the statistics.

At temperatures 0.8 and 1.0, no fundamental changes in the internal structure of the bilayer occur, and these systems rapidly equilibrate. However, at temperatures 1.2 and 1.4, the situation is different. The complicated trajectories indicate a long-range restructuring of the system, particularly at the temperature 1.4. The crystalline system initially dissolves into an disordered phase, and then the molecules begin to build a structure having a higher number of hydrophobic contacts. This phenomenon will be discussed in more detail below. The dissolution of the high-temperature system, at $T^* = 2.0$, is rapid, and the equilibration time

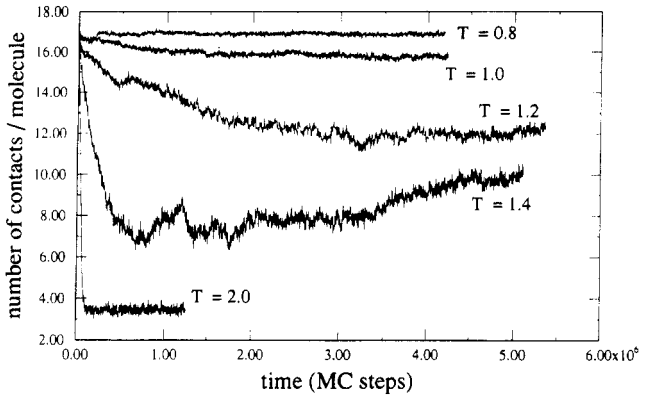

Figure 4. Trajectories of the average number of hydrophobic contacts for systems at different temperatures.

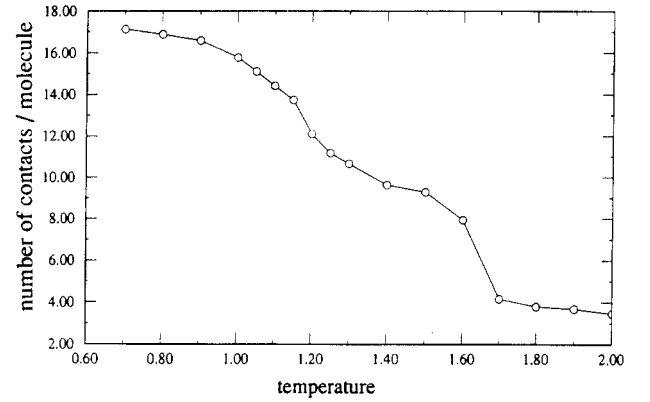

Figure 5. Mean number of hydrophobe–hydrophobe contacts as a function of reduced temperature.

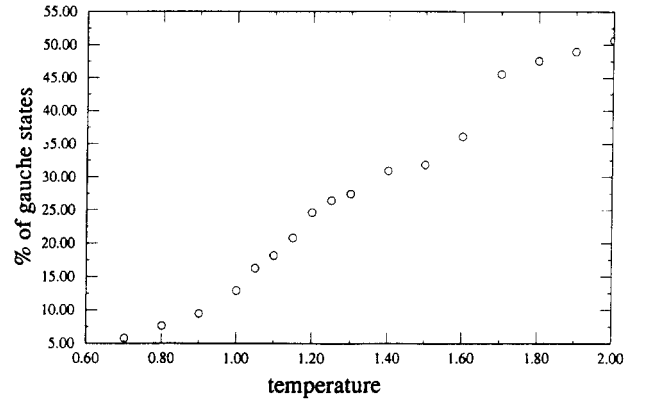

Figure 6. Percentage of "gauche" states as a function of temperature.

is very short. The final plateau corresponds to an isotropic solution with a minimal number of contacts between alkane chains.

The mean number of contacts between hydrophobic units and the percentage of "gauche" states have been calculated. Plots of these quantities as a function of reduced temperature are shown in Figures 5 and 6, respectively. Both quantities exhibit stepwise behavior between $T^* = 1.0$ and $T^* = 1.7$. Above the temperature $T^* = 1.0$, the number of contacts between hydrophobic beads falls drastically and the percentage of the "gauche" states increases. Then, above $T^* = 1.25$ both of the quantities are approximately stable, until the next jump which occurs above $T^* = 1.6$. The error in the observed values depends on temperature, but roughly, it is on level of the radius of the circles on the plots. These plots provide evidence that the dissolution of the model crystal occurs through at least two quasi-stable intermediate stages.

The character of these transitions is further investigated in Figure 7 where the heat capacity C_v as function of the temperature is shown. The heat capacity is obtained from its well-known relationship to the energy dispersion:

$$C_v = 1/k_B T^2(\langle E^2\rangle - \langle E\rangle^2) \quad (3)$$

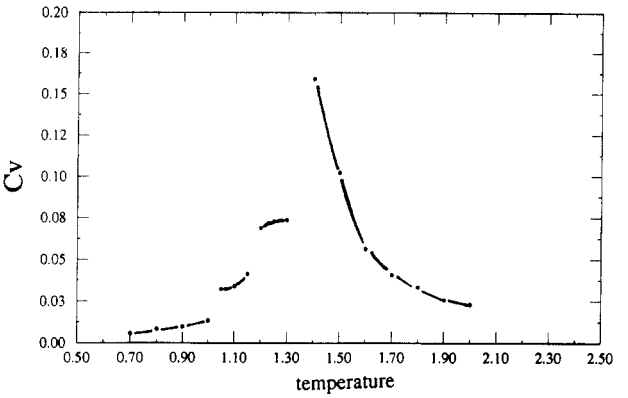

Figure 7. Heat capacity C_v as a function of the reduced temperature.

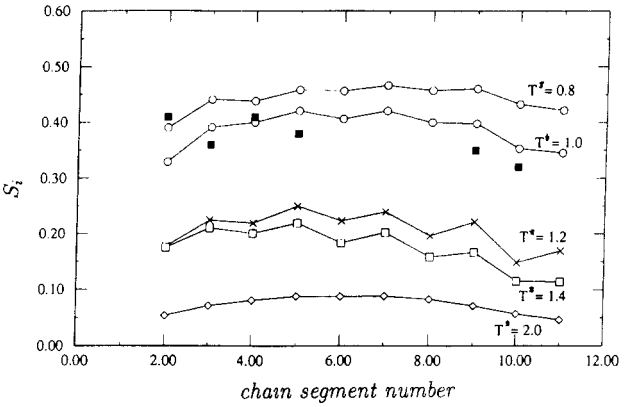

Figure 8. Segmental order parameter as a function of the number of carbon atoms for alkane chains at various temperatures. The solid squares denotes experimental data obtained from NMR (ref 25).

The character of the transitions is not so evident as in the previously depicted figures, and the level of error is much larger. Consistent with the mean number of contacts and the ratio of gauche states (Figures 5 and 6), the C_v curve has three characteristic points: near $T^* = 1.0$, $T^* = 1.2$, and $T^* = 1.5$. The first jump in C_v may be related to melting of the alkane chains, the second to the transition from the lamellar to the hexagonal phase, and the third to the homogenization of the lipid solution. It seems reasonable to ascribe the maximum in the C_v curve to the dissolution of the bilayer. However, given the complexity of this system and the scatter in the data, one cannot exclude the possibility that the heat capacity maximum is associated with the liquid-crystal to liquid transition within the bilayer and that the dissociation of the model membrane continuously occurs at a somewhat higher temperature.

The percentage of the "gauche" states is strictly connected with local ordering and chain stiffness. To obtain more precise information about ordering in the system, we have used both the order parameter calculated separately for each carbon site in the β- and γ-chains, S_i, and the mean order parameter for molecule, S_{mol}. S_i is defined analogous to liquid-crystal and bilayer systems (see e.g. ref 23)

$$S_i = \langle \tfrac{3}{2}\cos^2\theta_i - \tfrac{1}{2}\rangle \quad (4)$$

where θ_i is defined as an angle between the ith bond vector and the direction of the sum of both head-to-end vectors of the molecule. The origin is set at the branch point, and both hydrocarbon chains contribute to S_i. This definition of the local order parameter is consistent with the definition of the experimental CD bond order parameter S_{CD}, and[19]

$$S_{mol} = -2S_{CD} \quad (5)$$

The order parameter for the whole chain is the arithmetic average over the S_i. Figure 8 presents the segmental order parameter as a function of carbon position away from the branch point at some chosen temperatures. The shape and values of the order parameter are close to those obtained experimentally (using the EPR and

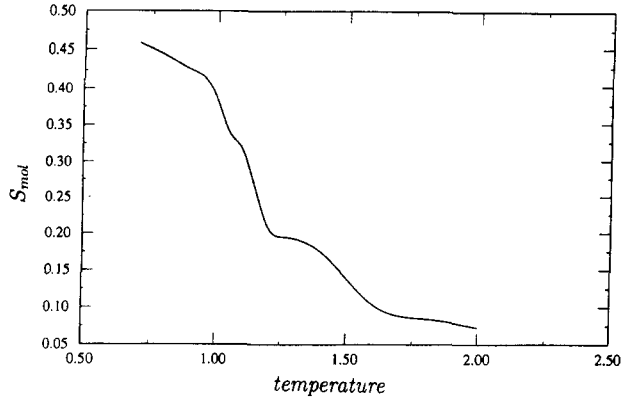

Figure 9. Mean order parameter as a function of the reduced temperature.

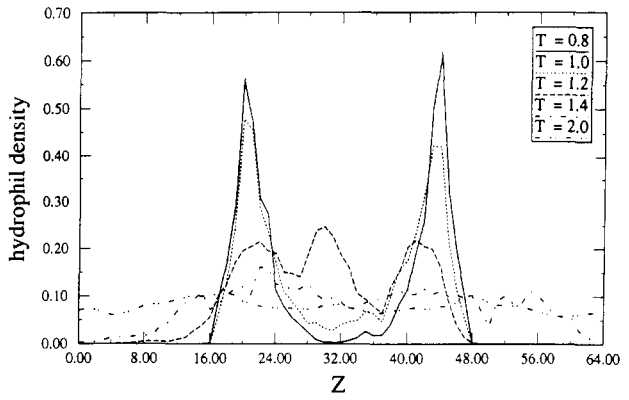

Figure 10. Density profiles of the hydrophils down the Z axis at various temperatures.

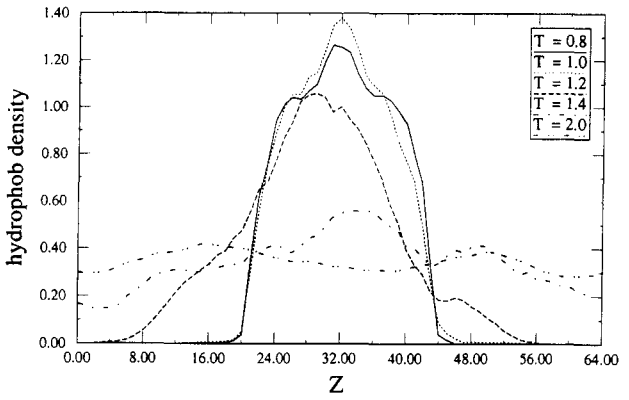

Figure 11. Density profiles of the hydrophobes down the Z axis at various temperatures.

NMR techniques[25,26]) and theoretically.[27,28] For comparison, experimental data for the segmental order parameter obtained using deuterium magnetic resonance for the lamellar phase of potassium laurate at T = 304 K[25] are superimposed (the solid squares). In the present work, we use the reduced temperature T^*, which is defined for computational convenience as the dimensionless ratio $T^* = k_BT/\epsilon_h$. The thermodynamic data for alkane–water systems can be used to give a rough idea about the relationship between the reduced temperature and the absolute temperature. The free energy of transfer from water to the alkane phase for alkane molecules equals 884 cal/mol per methylene group at T = 298 K.[19] The mean number of contacts per hydrophobe in our model bilayer structure equals 1.45, and the energy per single hydrophobe–hydrophobe contact equals k_BT. Therefore, the energy of transfer of a hydrophobic chain from the model "water" phase to the "bilayer" phase is equal to 1.45 per hydrophobe in reduced units. Thus, we estimate the absolute temperature: $T \propto$ 310 K. (Of course, the above scaling is valid only for temperatures below the temperature at which the model bilayer dissolves.) This equation gives the absolute temperature of the main transition between 300 and 310 K, which is close to the thermodynamic data for DLPE, 308.6 K.[19] We want to repeat once more that the estimate of the temperature is highly approximate (e.g., we have neglected the entropic contribution to free energy) and can only serve to give some insight into the nature of the reduced parameters we have employed.

Qualitative agreement of the experimental data on the segmental order parameter with the present simulations in the liquid bilayer region can be seen. This is suggestive that the MC simulation can give some information about the structure of water–lipid systems. The low simulated value of the segmental order for the beginning of the chain (close to the "head" of the molecule) seems to be an artifact arising from a too small volume of the model head group. The local density close to the surface of the model bilayer is much lower, and the mobility of this fragment is unnaturally high. Additionally, the initial oscillations in the order profile are due to the fact that the two lipid chains are nonequivalent in real phospholipids, a fact not considered in the present model.

Figure 9 displays the mean order parameter of the system, S_{mol}, as a function of temperature. S_{mol} exhibits the same stepwise character as was seen for the temperature dependence of the number of hydrophobic contacts and the percentage of gauche states. Figure 9 again shows that there are two transitions close to temperatures 1.2 and 1.5. However, unlike the previous plots, the first jump of S_{mol} is larger and sharper. This indicates that the transition from the liquid-crystal bilayer into a quasi-hexagonal phase is mainly connected with changes in the order rather than in the energy of the system. The shape of the curve is analogous to that obtained theoretically by Marcelja,[27] but the observed range of temperatures is much larger in our model.

On comparing the density profiles of hydrophils and hydrophobes down the Z axis (perpendicular to the bilayer surface), for temperatures T^* = 0.8, 1.0, and 1.6 (see Figures 10 and 11), we see that the transition is related to the change in the internal structure of the model bilayer. The bimodal distribution of the hydrophilic beads as well as the distribution of the hydrophobic ones is approximately stable up to the transition temperature, after which it changes drastically into a uniform distribution. At T^* = 1.0, one may note that the hydrophobic groups are still mostly inside the bilayer and the polar ones lie mostly on the surfaces. However, the α-chain beads (hydrophils) become more diffuse, and there is a nonzero probability of finding an α-chain inside the bilayer. Consequently, the process of slow interchange of α-chain positions between the two surfaces becomes possible. Indeed, this interchange process has been observed during the simulation. This flip-flop process was very rare, and we have observed only several occurrences per one cycle of simulation. The approximate time between the flip-flop transitions was 400 000 MC steps at T^* = 1.05 and 150 000 MC steps at T^* = 1.15. Finally, at a critical temperature, the bilayer dissociates. The curves at T^* = 1.4 show the situation after the complete dissolution of the model membrane. This is no longer an ordered structure but rather an irregular cluster containing a relatively high concentration of solvent.

Direct visualization of the same transition is shown in Figure 12, which presents representative snapshots of the system over a range of temperatures. At T^* = 0.8 (Figure 12a), the hydrocarbon chains are stiff and almost fully elongated, being packed according to a two-dimensional pattern. This order is partially destroyed at T^* = 1.0 (Figure 12b), where one can see many gauche defects in the hydrophobic chains. The chains are highly disordered, much like that in a liquid paraffin, but the average chain orientation is perpendicular to the bilayer surface. Moreover, this liquidlike bilayer is still stable and does not exhibit any tendency to completely dissolve. At the higher temperature T^*

(25) Mely, B.; Charvolin, J.; Keller, P. *Chem. Phys. Lipids* **1975**, *15*, 161.
(26) Davis, J. H. *Biophys. J.* **1979**, *27*, 339.
(27) Marcelja, S. *Biochim. Biophys. Acta* **1974**, *367*, 165.
(28) Ferrarini, A.; Nordio, P. L.; Moro, G. J.; Crepeau, R. H.; Freed, J. H. *J. Chem. Phys.* **1989**, *91*, 5707.

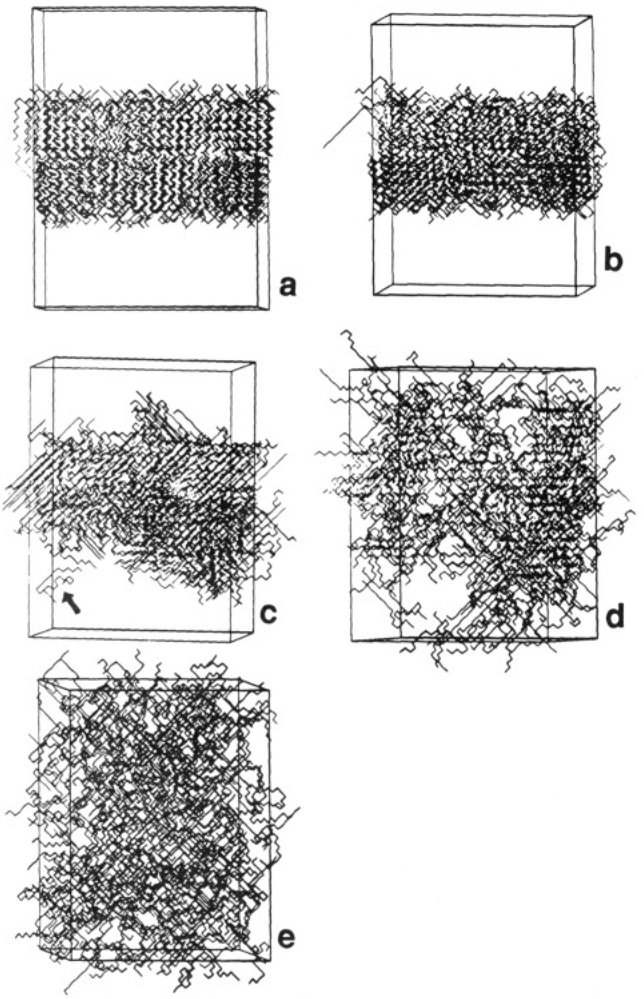

Figure 12. Snapshots of the system at various temperatures: (a) Lipid crystal at $T^* = 0.8$; the chains are stiff and are predominantly "trans". (b) Liquid bilayer at $T^* = 1.0$. The alkane chains are flexible, and there are many "gauche" states. The global ordering remains perpendicular to the bilayer surface. (c) Transition to a three-dimensional structure at $T^* = 1.2$. The molecules diffuse out of the bilayer (the arrow points to a "free floating" molecule). (d) Fragment of a stable, three-dimensional structure at $T^* = 1.4$. (e) Uniform solution at $T^* = 1.8$; the molecules are free-floating in the "water" solvent.

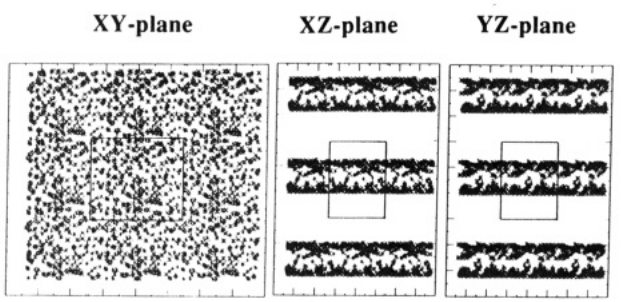

Figure 13. Schematic illustration of the structure of the system at $T^* = 1.0$. The positions of the hydrophilic branch points are shown as asterisks. The rectangle at the center of the picture contains "real" points, and the remainder of the points are periodic replicas. The system has strongly expressed bilayer structure.

= 1.2. (Figure 12c), the system begins to rearrange and the solvent "diffuses" into the membrane. The molecules partially change orientation; they can now diffuse out of bilayer and return. The arrow points to a "free-floating" lipid molecule outside the bilayer. The reordering transition is almost finished by $T^* = 1.4$ (Figure 12d), where the lipid molecules form a nonbilayer structure; unfortunately, the MC box appears to be too small to obtain a better defined structure. At $T^* = 1.8$ (Figure 12e), the system looks like a uniform, paraffin liquid.

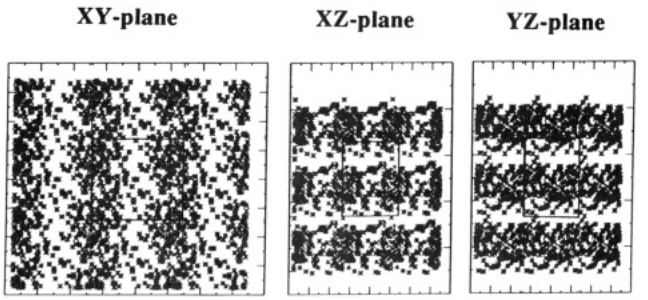

Figure 14. As in Figure 13, an illustration of the structure of the system but at $T^* = 1.4$. The heads are organized into a three-dimensional structure, analogous to that in a hexagonal II phase.

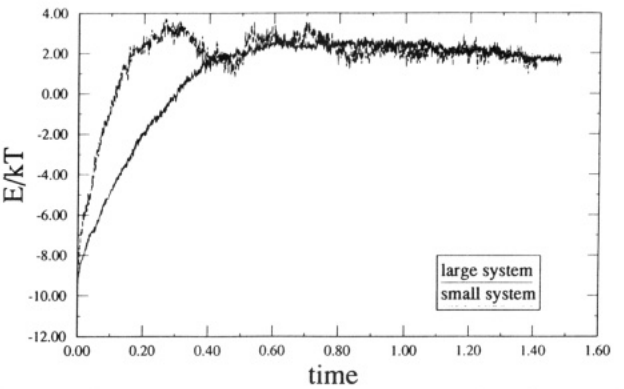

Figure 15. Comparison of plots of the energy per bead as a function of temperature for systems comprised of 230 and 920 molecules. The 920-molecule system starts out at lower values.

To provide additional information about the structure of the lipid–water system, Figures 13 and 14 present schematic pictures of the system, where only the branch points of the model molecules are shown. These pictures are obtained by projecting the Cartesian coordinates of the branch points onto *XY*, *XZ*, and *YZ* surfaces. Figure 13 shows the system at temperature $T^* = 1.0$, and Figure 14 shows the same system at $T^* = 1.4$. In all the pictures, the rectangle bounded by lines in the center contains the "real" points; the additional points are periodic images of the MC box. The $T^* = 1.0$ system exhibits very distinctive bilayer properties. It is periodic along the *Z* axis direction and homogeneous in the *XY* plane. The $T^* = 1.4$ system has a somewhat more complicated structure. The hydrophilic heads of the model lipids are organized into cylindrical structures, similar to those in the hexagonal II phase[5,6,29] and analogous to those obtained by Larson[14] for a system of amphiphilic molecules, using quite different methods. This effect is consistent with the minimum in the head group mobility near this temperature (see Table I). The head groups are much more closely packed in this structure. The local density near the heads is higher, and the probability of acceptance of the move decreases because of steric problems. It seems that the dimensions of the MC box are too small to achieve a full structural transition, but the system has an evident tendency to adopt cylindrical symmetry.

To test the effect of the periodic boundary conditions on the properties of the system, we have generated a system in a MC box that is 2 times larger in the *X* and *Y* directions ($96 \times 96 \times 64$). The system, containing 920 lipid molecules with the same surface density 0.8, was equilibrated at the temperature $T^* = 1.4$. Figure 15 shows the energy of the system as a function of the simulation time. For comparison, the analogous curve for the "small" (230 molecules) system is shown in the same figure. As one can see, the change in dimensions of the MC cube leaves the dynamics and the energetic properties of the system unaffected. The large system behaves exactly the same as the small one, and the equilibrium energies of both systems are very close. However,

(29) Gordon-Kamm, W. J.; Steponkus, P. L. *Proc. Natl. Acad. Sci. U.S.A.* **1984**, *81*, 6373.

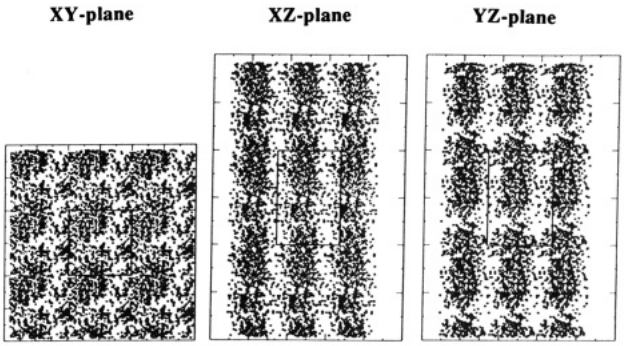

Figure 16. Schematic illustration of the structure of the system of 920 lipid molecules. The asterisks represent positions of the hydrophobic branch points of the model lipid molecule. As in Figure 13, the rectangles in the central region of the figures represent molecules in the MC box, and the remainder of the points are periodic replicas.

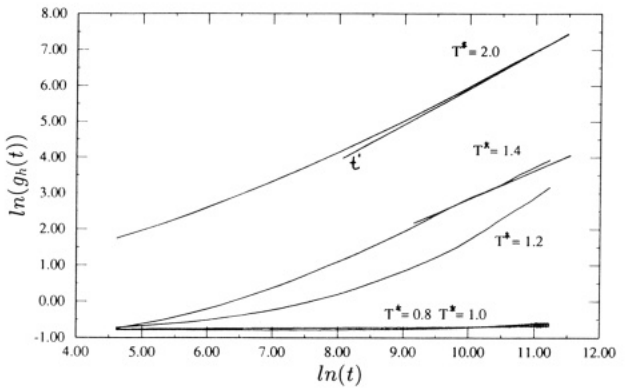

Figure 17. log–log plots of mean-square displacement of the branch point of the model molecule as a function of time for $T^* = 0.8$, 1.0, 1.2, 1.4, and 2.0.

the dimensions of the lamellar structures in the large system are still on the scale of length of the edge of the MC box (Figure 16). This provides evidence that the distance scale of the structural transition at this temperature is much larger than the size of the MC box. Consequently, because of the boundary conditions of the model, the system cannot achieve its equilibrium structure in a nonbilayer phase. Unfortunately, our computer resources are inadequate to explore a system having larger dimensions. The effect of the boundary condition is less distinct in the bilayer phase, and we would expect that structure of this phase is close to equilibrium. This problem was discussed above in connection with discussion of the efficiency of the algorithm.

3.2. Dynamic Properties. We next turn to a brief examination of the dynamics exhibited by these systems. The mean-square displacements of the branch point (head) and both ends of the alkane chains were calculated for the simulated systems according to

$$g_i(t) = \langle [r_i(t) - r_i(0)]^2 \rangle \qquad (6)$$

where i denotes the head or end point and $r_i(t)$ are the Cartesian coordinates of the head or end of the lipid molecule at time t.

The mean-square displacement of the branch point, $g_h(t)$, as a function of time is plotted in Figure 17. As expected, the dynamics depend strongly on temperature. At low temperature, the dynamics is very restricted, and the simulation is too short to cross over into the free diffusion regime. The dynamics of the nonbilayer phase and the dissolved (isotropic) system is analogous to the dynamics of dense polymer systems. At large times, the free diffusion limit is achieved, where the mean-square displacement is proportional to time.

A difference between the dynamic properties of the heads and tails of the model molecules can be observed in Figure 18, where a log–log plot of the mean-square displacements of the heads and the ends of the alkane chains as a function of time is presented. The situation is similar to that seen in the cases of a polymer

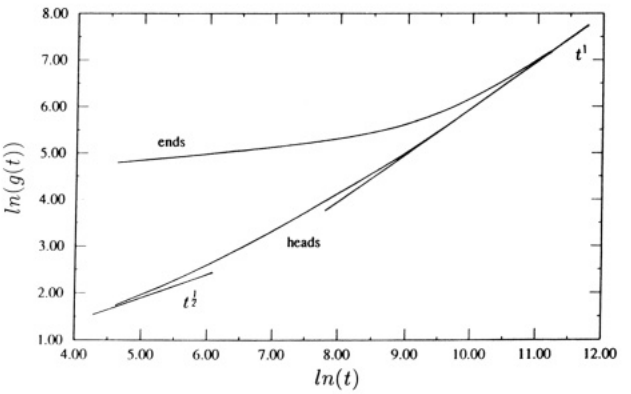

Figure 18. log–log plot of mean-squared displacements of the branch points (heads) and ends of the alkane chains at $T^* = 2.0$.

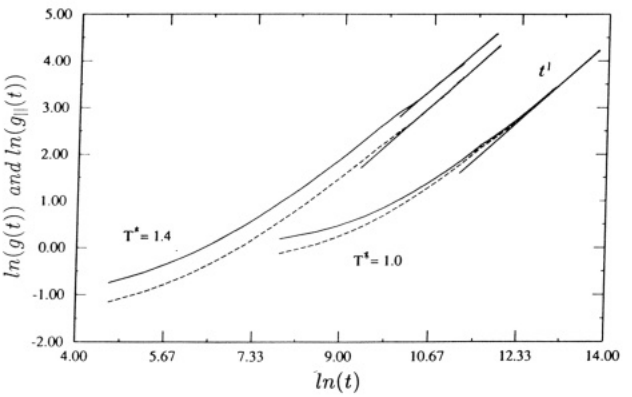

Figure 19. log–log plot of mean-square displacement, $g(t)$ (solid curve), and lateral mean-squared displacement, $g_\parallel(t)$ (dashed curve), of the heads of the model lipid molecules at $T^* = 1.0$ (bilayer phase) and at $T^* = 1.4$ (hexagonal phase).

melt[30,31] and when molecules are constrained to lie near an interface.[16] The ends are always more mobile than heads, but in the intermediate time region, where $g_e(t)$ is of the range of length of the chain, the mobility of the ends slows down. This is an effect of the slower initial dynamics of the branching point (head), which must have time to overtake the end. After this time, both curves coalesce and reach the free diffusion regime.

An important feature of natural membranes is the lateral diffusion of lipids in the bilayer plane. To examine this effect in our model, the two-dimensional mean-square displacement was calculated:

$$g_\parallel(t) = \langle (x(t) - x(0))^2 + (y(t) - y(0))^2 \rangle \qquad (7)$$

The log–log plot of $g_\parallel(t)$ (dashed lines) and, for comparison, the three-dimensional $g(t)$ (solid lines) for these same systems are shown in Figure 19. The solid line denotes ln ($g(t)$) and the dashed, ln ($g_\parallel(t)$). For the bilayer phase, at a temperature $T^* = 1.0$, both curves are distinguishable at small displacements. The difference between them is roughly equal ln $^3/_2$, which is the characteristic value for isotropic systems. As the total displacement increases, the lateral displacement component begins to prevail, and finally, at distances larger than 5–7 lattice units, only lateral diffusion exists. The system reaches the free diffusion regime, but only in two dimensions. This is very suggestive of the existence and stability of the lipid bilayer phase in this model.

At a slightly higher temperature, which is associated with the quasi-hexagonal phase, both curves never coalesce, and the difference between them is close to ln $^3/_2$. This provides additional evidence for the existence of a stable, nonbilayer phase in the present model.

The random walk in the dynamic Monte Carlo method is governed by a master equation,[32] and there is no strict relation

(30) Kolinski, A.; Skolnick, J.; Yaris, R. *J. Chem. Phys.* **1987**, *86*, 7164.
(31) Skolnick, J.; Kolinski, A. *Adv. Chem. Phys.* **1990**, *78*, 223.

between the simulation time measured in MC steps and physical time. The time scale of the process is a function of the transition probability in the simulation and depends on density, temperature, and potentials defined in the model. Therefore, the time-dependent properties in the present model have a rather qualitative character. However, comparison of lattice MC model with an analogous Brownian dynamics model[33] suggests that 1 MC step in the present simulation is on the order of the mean isomerization time (0.1–1 ns).

4. Discussion

Real lipid bilayer systems can undergo many phase transitions, and the phase diagram for the lipid–water system is very complicated. From the point of view of the present simple lattice model, the important question is which properties of the real bilayer system can be reproduced. We find that a transition from a low-temperature, quasi-crystalline phase to a fluid phase (chain melting) can be observed in the present diamond lattice model. In the literature, this transition is postulated to be first order,[19,20] but in the lattice model, the energy change is relatively smooth and the transition appears to be of higher order. This may be due to the inadequacy of the representation of interchain interactions and/or the fact that we have simulated systems that are too small. On the other hand, other theoretical treatments claim that this is a higher order transition (ref 20 and references cited therein); clearly, more work remains to be done. At this point, it appears that there is a transition associated with a jump in the overall ordering of the system which is accompanied by the presence of a substantial change in the lateral diffusion rate of the lipid molecules. Because of the finite size of the present model, the order of this very cooperative transition cannot be assessed.

The transition from the fluid bilayer to one of the hexagonal phases appears to be a complicated, large-scale transition. This requires reorganization of a large collection of lipid molecules, accompanied by change in the symmetry of the entire system. At this time, the complete simulation of this transition is beyond our computational capabilities. The quasi-hexagonal system obtained here is not fully at equilibrium and is partially predefined by the presence of periodic boundary conditions.

The formation of the nonbilayer phase proceeds via the partial dissolution of the bilayer, with a concomitant change in the system order and diffusion of "water" molecules (represented by empty lattice points) into the bilayer. Than, after some time, a self-reorganization of the system begins. The local ordering as well as the number of chain–chain contacts increases, and a new system with different structure and symmetry develops.

The process of dissolution of the nonbilayer system is very fast. After reaching the transition temperature, at about $T^* = 1.5$, the system becomes a homogeneous solution, and the number of interchain contacts substantially decreases.

5. Conclusion

We have developed a lattice Monte Carlo model of a lipid–water system on the level of the unified-atom representation of lipid molecules. The model gives a qualitative description of the properties of the water–lipid systems over a wide temperature range. In particular, we find the existence of phase transitions from the gel to the liquid bilayer and from the liquid bilayer to the hexagonal phase and finally the dissolution of the lipid structures.

The model is in good accord with mean field calculations and experiments for the liquid bilayer phase. Values of the segmental and global ordering and the fraction of gauche states agree semiquantitatively with experimental NMR data. An advantage of the present model is the possibility of exploring the dynamic properties of the system. The existence of lateral diffusion in the liquid bilayer and a free-diffusion regime in the nonbilayer phases was established. In forthcoming work, we will also present a more detailed analysis of the intermediate time dynamics exhibited by this model.

The model described here forms the basis of an ongoing exploration of more detailed problems associated with the thermodynamics of lipid–water systems. Further examination of the main phase transition in the bilayer (the gel–liquid bilayer transition) is clearly required. The character and order of this transition remain controversial, and it is possible that this simple but well-defined model can provide additional insights. Another possibility is to use the model to examine the problem of self-organization in lipid systems. This requires the use of large assemblies of lipid molecules and long simulation times, and this lattice model may be very appropriate for the qualitative examination of this very important problem. Some confidence that we can accomplish aspects of this is provided by the example of the rearrangement of the lipid molecules into a three-dimensional, nonbilayer phase seen in the present preliminary simulations.

The possibility of examining the nature of lipid–protein interactions and the folding pathways of short membrane proteins are natural extensions of the present work. These calculations require the use of very large systems of molecules and much more complicated interactions but are tractable on the level of this lattice model. These areas will be the subject of future publications.

In parallel to this simplified lattice based approach, we are working on making the model more realistic by using a hierarchy of models—from lattice Monte Carlo to off-lattice Monte Carlo—and finally performing molecular dynamics simulations. The present model will be a very efficient generator of equilibrium systems at various densities and temperatures; this will allow us to study the nature of the local dynamics in more detail.

Acknowledgment. This research is supported in part by a grant from the National Institutes of Health, GM37408. Stimulating conversations with Prof. Antonio Rey are gratefully acknowledged. We thank the referees for their very helpful comments.

(32) Mouritsen, O. G. In *Molecular Description of Biological Membranes by Computer Aided Conformational Analysis*; Brasseur, R., Ed.; CRC Press: Boca Raton, FL, 1990.

(33) Rey, A.; Skolnick, J. *Chem. Phys.* **1991**, *158*, 199.